UCHEP-04-04

B DECAYS TO OPEN AND HIDDEN CHARM AT BELLE

A. DRUTSKOY

Physics Department, University of Cincinnati,
345 College Court, Cincinnati, OH 45221, USA

The recent Belle collaboration measurements of B decays to open and hidden charm are discussed. Color-suppressed decay branching fractions are measured with an improved accuracy. The branching fractions of the $\bar{B}^0 \to D_s^+ K^-$ and $\bar{B}^0 \to D_s^- \pi^+$ decays, measured with improved accuracy, and $\bar{B}^0 \to D_{sJ}^+ K^-$ and $\bar{B}^0 \to D_{sJ}^- \pi^+$ decays, measured for the first time, are compared. The two-body invariant masses of the three-body $B^0 \to D^{(*)0}\pi^+\pi^-$ and $B^0 \to J/\Psi\pi^+\pi^-$ decays are studied.

1 Results

1.1 Color-suppressed $\bar{B}^0 \to D^0\pi^0(/\omega/\eta)$ and $\bar{B}^0 \to D^{(*)0}\eta'$ decays

The weak decays $\bar{B}^0 \to D^{(*)0}h^0$, where h^0 represents a light neutral meson, are usually described by a "color-suppressed" diagram as shown in Fig.1.

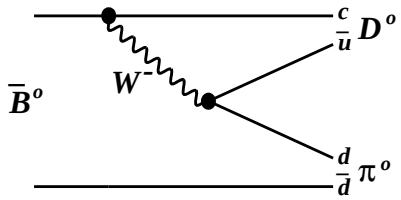

Figure 1. Color-suppressed diagram for the decay $\bar{B}^0 \to D^{(*)0}\pi^0$.

Within "naïve" factorization models [1,2], the color-matching requirement leads to branching fractions in the range (0.3-1.7)$\times 10^{-4}$. However previous measurements by the CLEO [3], Belle [4] and BaBar [5] collaborations were substantially shifted to the larger values (2-4)$\times 10^{-4}$. The new Belle measurements are based on a larger data sample of 140 fb^{-1}. This corresponds to a seven-fold increase over the previous Belle measurement and almost twice that of the earlier BaBar measurement. With increased statistics a more detailed study of continuum and $B\bar{B}$ related backgrounds was done, reducing systematic uncertainties.

The Belle measurements of these branching fractions for each decay mode is shown in Table 1.

Table 1. B branching fractions for color-suppressed decays.

Decay mode	Br. Fraction ($\times 10^{-4}$)
$\bar{B}^0 \to D^0\pi^0$	$2.31 \pm 0.12 \pm 0.23$
$\bar{B}^0 \to D^0\eta(\gamma\gamma)$	$1.77 \pm 0.18 \pm 0.20$
$\bar{B}^0 \to D^0\eta(\pi^0\pi\pi)$	$1.89 \pm 0.29 \pm 0.20$
$\bar{B}^0 \to D^0\eta$	$1.83 \pm 0.15 \pm 0.27$
$\bar{B}^0 \to D^0\omega(\pi^0\pi\pi)$	$2.25 \pm 0.21 \pm 0.28$
$\bar{B}^0 \to D^0\eta'$	$1.17 \pm 0.20\ ^{+0.10}_{-0.14}$
$\bar{B}^0 \to D^{*0}\eta'$	$1.23 \pm 0.34 \pm 0.21$

These branching fractions are about one-two standard deviations lower than the BaBar measurements but higher than early predictions within factorization models. The latter discrepancy may be explained by additional contributions from final state rescattering or non-factorisable diagrams.

1.2 Improved measurement of $\bar{B}^0 \to D_s^+ K^-$ and $\bar{B}^0 \to D_s^- \pi^+$ decays and first study of $\bar{B}^0 \to D_{sJ}^+ K^-$ and $\bar{B}^0 \to D_{sJ}^- \pi^+$ decays

The decays $\bar{B}^0 \to D_{s(J)}^+ K^-$ are of special interest because the quark content of the initial $\bar{B}^0$ meson $(b\bar{d})$ is completely differ-

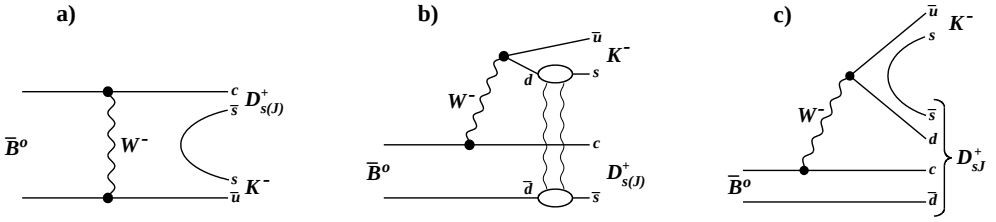

Figure 2. Diagrams describing $\overline{B}^0 \to D^+_{sJ}K^-$ decay.

ent from that of the $D^+_{s(J)}K^-$ final state ($cs\bar{s}\bar{u}$), indicating an unusual configuration with both initial quarks involved in the weak decay. Branching fractions with the D^+_s meson $\mathcal{B}(\bar{B}^0 \to D^+_s K^-) = (4.6^{+1.2}_{-1.1} \pm 1.3) \cdot 10^{-5}$ and $(3.2 \pm 1.0 \pm 1.0) \cdot 10^{-5}$ have been measured by the Belle [6] and BaBar [7] collaborations, respectively. Predictions of this branching fraction have been obtained assuming a dominant contribution from a PQCD factorization W exchange process [8,9] (Fig. 2a) or, alternatively, from final state interactions [10,11] (Fig. 2b), and range from a few units of 10^{-6} to 10^{-4}. If the D_{sJ} mesons have a four-quark component then the tree diagram with $s\bar{s}$ pair creation (shown in Fig. 2c) may also contribute.

The decay mode $\bar{B}^0 \to D^-_{s(J)}\pi^+$ can be described by a "b to u" tree diagram. Within the factorization approach[12] the branching fraction ratio $R_{\pi^+/D^+} = \mathcal{B}(\bar{B}^0 \to D^-_s\pi^+)/\mathcal{B}(\bar{B}^0 \to D^-_s D^+)$ is predicted to be $(0.424 \pm 0.041) \cdot |V_{ub}/V_{cb}|^2$ and can be used to obtain the ratio of Cabbibo-Kobayashi-Maskawa matrix elements $|V_{ub}/V_{cb}|$.

The B decay channels with the pseudoscalar D_s meson were studied using 253 fb^{-1} of data ($275 \times 10^6 B\bar{B}$ pairs), whereas channels with the D_{sJ} were studied using 140 fb^{-1} of data (152×10^6 $B\bar{B}$ pairs). D^+_s mesons are reconstructed in the $\phi\pi^+$, $K^{*0}K^+$ and $K^0_S K^+$ decay channels. D_{sJ} mesons are reconstructed in the $D^*_{sJ}(2317)^+ \to D^+_s\pi^0$ and $D_{sJ}(2460)^+ \to D^+_s\gamma$ decay modes.

The D_s mass distributions in the B signal region are shown in Fig. 3. The points are experimental data and the curves display the fit results. In addition to clear signals at the D^+_s mass in Fig. 3, the D^+ mass peak (D^+ decays in the same final states) is also seen.

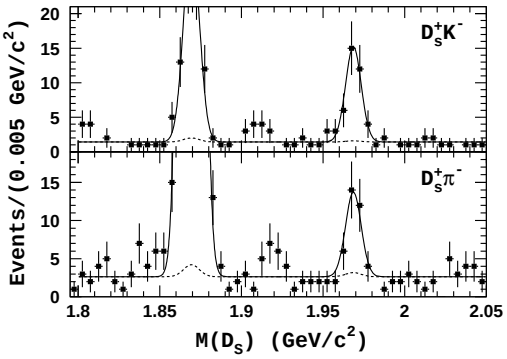

Figure 3. $M(D_s)$ spectra for $\bar{B}^0 \to D^+_s K^-$ (top) and $\bar{B}^0 \to D^-_s\pi^+$ (bottom) in the B signal region.

The branching fractions obtained from the fits are $\mathcal{B}(\bar{B}^0 \to D^+_s K^-) = (2.93 \pm 0.55 \pm 0.79) \cdot 10^{-5}$ and $\mathcal{B}(\bar{B}^0 \to D^-_s\pi^+) = (1.94 \pm 0.47 \pm 0.52) \cdot 10^{-5}$. These agree within errors with the previous measurements.

The $\Delta M(D_{sJ})$ distributions in the B signal region for various $D^+_{sJ}K^-$ and $D^-_{sJ}\pi^+$ combinations are shown in Fig. 4. A clear $\bar{B}^0 \to D^*_{sJ}(2317)^+K^-$ signal is observed; no significant signals are observed in the remaining modes.

For the $\bar{B}^0 \to D^*_{sJ}(2317)^+K^-$ decay, the product branching fraction is measured to be

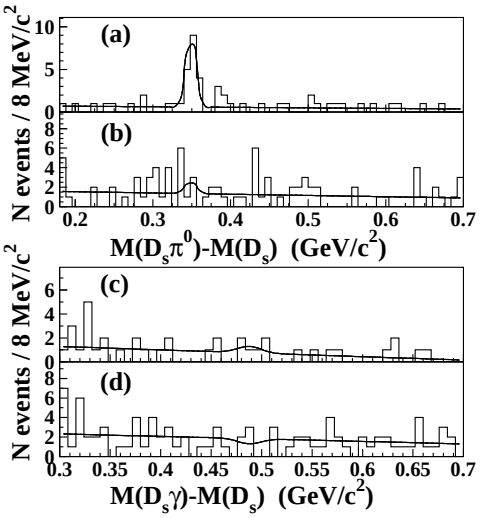

Figure 4. The $\Delta M(D_{sJ})$ distributions in the B signal region for the (a) $D^*_{sJ}(2317)^+K^-$, (b) $D^*_{sJ}(2317)^-\pi^+$, (c) $D_{sJ}(2460)^+K^-$ and (d) $D_{sJ}(2460)^-\pi^+$ combinations are shown.

$\mathcal{B}(\bar{B}^0 \to D^*_{sJ}(2317)^+K^-) \times \mathcal{B}(D^*_{sJ}(2317)^+ \to D_s^+\pi^0) = (5.3^{+1.5}_{-1.3} \pm 0.7 \pm 1.4) \cdot 10^{-5}$. Recent measurements imply that the $D^*_{sJ}(2317)^+ \to D_s^+\pi^0$ channel is dominant and the $D_{sJ}(2460)^+ \to D_s^+\gamma$ fraction is around 30%. Taking into account these approximate values, we can conclude that $\mathcal{B}(\bar{B}^0 \to D^*_{sJ}(2317)^+K^-)$ is of the same order of magnitude as $\mathcal{B}(\bar{B}^0 \to D_s^+K^-)$, but at least a factor two larger than the $\bar{B}^0 \to D_{sJ}(2460)^+K^-$ branching fraction, in contrast to the naïve expectation that decays with the same spin-doublet $D^*_{sJ}(2317)^+$ and $D_{sJ}(2460)^+$ mesons would have similar rates. It is interesting to mention, that the ratio of $\mathcal{B}(B \to D^*_{sJ}(2317)^+D)$ and $\mathcal{B}(B \to D_s^+D)$ decay branching fractions [13] is approximately 1/10, indicating to a different behaviours of the $B \to D_sK$ and $B \to D_sD$ processes [14].

1.3 Study of $B^0 \to D^{(*)0}\pi^+\pi^-$ decays

The three-body $B^0 \to D^{(*)0}\pi^+\pi^-$ decays were studied with 140 fb^{-1} of data. These processes can provide important information about intermediate two-body resonances. The $D^0\pi^+$ and $D^{*0}\pi^+$ mass distributions are shown in Figs. 5,6. Points are experimental data, the hatched histogram is obtained using sideband events and the open histogram is MC simulation with all intermediate resonances included. The masses and widths of narrow ($\leq$100 MeV/c^2) D^{**} resonances observed are listed in Table 2. These values are in a good agreement with predictions obtained within potential models [15].

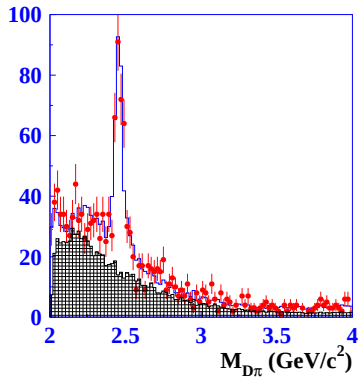

Figure 5. The $D^0\pi^+$ mass distribution.

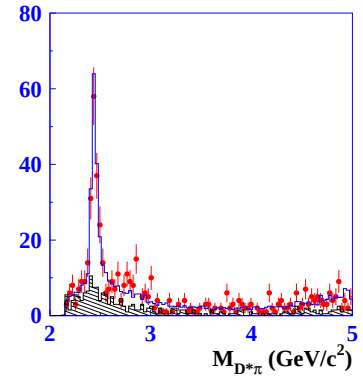

Figure 6. The $D^{*0}\pi^+$ mass distribution.

The quasi-two-body $\bar{B}^0 \to D^{**+}\pi^-$ final state branching fractions were measured and compared to results obtained by the Belle collaboration in the studies of the charged $B^+ \to D^{(*)-}\pi^+\pi^+$ decay modes [16]. The branching fractions obtained for the narrow resonances are similar for the neutral and

Table 2. Masses and widths of narrow D^{**} resonances.

Parameter	Value, MeV/c^2
$M(D_2^{*+})$	$2459.5 \pm 2.3 \pm 0.7\ ^{+4.9}_{-0.5}$
$\Gamma(D_2^{*+})$	$48.9 \pm 5.4 \pm 4.2 \pm 1.9$
$M(D_1^{+})$	$2428.2 \pm 2.9 \pm 1.6 \pm 0.6$
$\Gamma(D_1^{+})$	$34.9 \pm 6.6\ ^{+4.1}_{-0.9} \pm 4.1$

charged B decays.

1.4 Study of $B^0 \to J/\Psi\pi^+\pi^-$ decays

The decay $B^0 \to J/\Psi\rho^0$ is governed by the $b \to c\bar{c}d$ transition and can exhibit a CP-violating asymmetry. In contrast to the $b \to c\bar{c}s$ transition, the $b \to c\bar{c}d$ process has substantial contributions from both the tree and penguin amplitudes, which could lead to different CP asymmetries of these processes. Thus, $B^0 \to J/\Psi\rho^0$ decays play an important role in probing non-tree diagram contributions.

The resonant structure of the $\pi^+\pi^-$ invariant mass spectrum from $B^0 \to J/\Psi\pi^+\pi^-$ decays was studied using 140 fb^{-1} of data. Five types of events are considered in the fit shown in Fig. 7: (i) $B^0 \to J/\Psi\rho^0$; (ii) $B^0 \to J/\Psi f_2$; (iii) $B^0 \to J/\Psi\pi^+\pi^-$ (non-resonant); (iv) $B^0 \to J/\Psi K_S^0$ (background) and (v) combinatorial background. The branching fractions obtained are $\mathcal{B}(B^0 \to J/\Psi\rho^0) = (2.8\pm0.3\pm0.3)\times10^{-5}$ and $\mathcal{B}(B^0 \to J/\Psi f_2) = (9.8 \pm 3.9 \pm 2.0) \times 10^{-6}$. The statistical significance of the latter is 2.9σ, and an upper limit is also set: $\mathcal{B}(B^0 \to J/\Psi f_2) < 1.5\times10^{-5}$ at 90% C.L. An upper limit is also set on the non-resonant channel: $\mathcal{B}(B^0 \to J/\Psi(\pi^+\pi^-)_{non-res.}) < 1.0 \times 10^{-5}$ at 90% C.L.

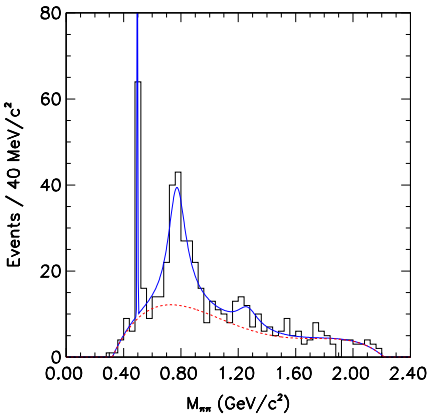

Figure 7. The distribution of $M_{\pi^+\pi^-}$ for $B^0 \to J/\Psi\pi^+\pi^-$ decay. Points are the experimental data. The solid line shows the result of fit with the K_S^0, ρ^0, f_2 and background contributions included, the dashed line is for the background contribution only.

References

1. M. Neubert and A.A. Petrov, *Phys. Lett.* B **519**, 50 (2001).
2. A. Deandrea and A.D. Polosa, *Eur. Phys. Jour.* C **22**, 677 (2002).
3. CLEO Collaboration, T.E. Coan *et al.*, *Phys. Rev. Lett.* **88**, 062001 (2002).
4. Belle Collaboration, K. Abe *et al.*, *Phys. Rev. Lett.* **88**, 052002 (2002).
5. BaBar Collaboration, B. Aubert *et al.*, *Phys. Rev.* D **69**, 032004 (2004).
6. Belle Collaboration, P. Krokovny *et al.*, *Phys. Rev. Lett.* **89**, 231804 (2002).
7. BaBar Collaboration, B. Aubert *et al.*, *Phys. Rev. Lett.* **90**, 181803 (2003).
8. D. Du, L. Guo, D.-X. Zhang, *Phys. Lett.* B **406**, 110 (1997).
9. C.D. Lu, hep-ph/0305061.
10. C.-K. Chua, W.-S. Hou, K.-C. Yang, *Phys. Rev.* D **65**, 096007 (2002).
11. B. Blok, M. Gronau, J.L. Rosner, *Phys. Rev. Lett.* **78**, 3999 (1997).
12. C.S. Kim, Y. Kwon, J. Lee, W. Namgung, *Phys. Rev.* D **63**, 094506 (2001).
13. Belle Collaboration, P. Krokovny *et al.*, *Phys. Rev. Lett.* **91**, 262002 (2003).
14. C.-H. Chen, H.-n Li, *Phys. Rev.* D **69**, 054002 (2004).
15. S. Godfrey and R. Kokoski, *Phys. Rev.* D **43**, 1679 (1991).
16. Belle Collaboration, K. Abe *et al.*, *Phys. Rev.* D **69**, 112002 (2004).